Journal of Solid State Chemistry 210 (2013) 116–120

Contents lists available at ScienceDirect

Journal of Solid State Chemistry

journal homepage: www.elsevier.com/locate/jssc

Fabrication and temperature-dependent magnetic properties of one-dimensional multilayer Au–Ni–Au–Ni–Au nanowires

S. Ishrat [a,d], K. Maaz [a,c], Kyu-Joon Lee [b], Myung-Hwa Jung [b,*], Gil-Ho Kim [a,*]

[a] School of Electronic and Electrical Engineering and Sungkyunkwan Advanced Institute of Nanotechnology (SAINT), Sungkyunkwan University, Suwon 440-746, Republic of Korea
[b] Department of Physics, Sogang University, Seoul 121-742, Republic of Korea
[c] Nanomaterials Research Group, Physics Division, PINSTECH, Nilore, Islamabad, Pakistan
[d] Department of Physics, COMSATS Institute of Information Technology, Lahore 54000, Pakistan

ARTICLE INFO

Article history:
Received 26 August 2013
Received in revised form
24 October 2013
Accepted 2 November 2013
Available online 11 November 2013

Keywords:
Nanostructured materials
Anisotropy
Magnetic measurements

ABSTRACT

Multilayer Au–Ni–Au–Ni–Au nanowires with a controlled diameter of ~100 nm were synthesized by electrochemical deposition in porous alumina templates. The length of each Ni-segment was controlled up to ~230 nm, while the length of the Au segment sandwiched between two Ni segments was ~180 nm. X-ray diffraction patterns and energy-dispersive X-ray spectra confirmed the formation of purely crystalline nanowires. The magnetic properties of the multilayer Au–Ni–Au–Ni–Au nanowires were investigated in the temperature range 2–300 K. Room-temperature magnetic hysteresis confirmed the ferromagnetic nature of the nanowires. The plot of coercivity as a function of temperature (from 2 to 300 K) followed law applicable for ferromagnetic nanostructures. The magnetization tended to increase as the temperature decreased, following the modified Bloch's law similar to ferromagnetic nanoparticles.

1. Introduction

In the past decade, nanoscale magnetic materials have attracted much attention because of their unique magnetic properties and potential applications in nanotechnology. The magnetic properties of nanostructured materials are usually controlled by their size, dimensions, and morphology. One-dimensional magnetic nanowires are very promising candidates for a variety of applications in medical devices, magnetic storage devices, and spintronics devices [1–5].There is a variety of hosting templates that can be used for the growth of one-dimensional nanostructures, such as alumina templates (AAO), mesoporous silica or porous silicon, and nuclear-track-etched polymer membranes [6]. As compared to other templates, AAO templates have a high density, chemical stability, and highly ordered porous structure that makes them suitable for the fabrication of segmented nanowires.

Magnetic nanostructures can be produced using different techniques, among which electrochemical deposition is very common and easily achievable at room temperature [3]. Template-assisted electrochemical deposition, which involves the reduction of ferromagnetic and nonmagnetic electrolytes at room temperature, is the best technique for the fabrication of multilayer nanowires [7,8]. These wires can be electrodeposited by alternately changing the electrolytes during deposition, and the length of each segment can be tuned by controlling the time and charge deposited during the deposition.

Magnetic characterization of diameter-modulated nanowires is necessary before they can be used in various potential spintronics applications. Multilayer ferromagnetic (Ni) and nonmagnetic (Au) nanowires are of growing interest because of their tuneable magnetic properties [9]. Although the magnetic properties of multilayer nanowires have been studied widely, the magnetic properties of diameter-modulated multilayer nanowires with beadlike structures have rarely been reported [10,11].

Recently, magnetic nanoparticles have great impact in the development of nanotechnology. Due to their extremely low sizes, and interaction among the constituents, the chain of magnetic nanoparticles often exhibit new and enhanced properties as compared to their bulk counterparts. There are several techniques that have been developed to obtain the ordered magnetic arrays of nanoparticles, including spin coating, vertical depositions, deposition on the patterned substrate, and applying external electric fields. However the arrays of nanoparticles grown by electrochemical deposition have rarely been reported earlier.

Diameter-modulated multilayer nanowires have interesting ferromagnetic ordering. For such nanowires, the core refers to the inner part of the nanoparticle, and the shell refers to the spin-glass surface

* Corresponding authors: School of Electronic and Electrical Engineering and Sungkyunkwan Advanced Institute of Nanotechnology (SAINT), Sungkyunkwan University, Suwon 440-746, Korea.
E-mail addresses: mhjung@sogang.ac.kr (M.-H. Jung).
ghkim@skku.edu (G.-H. Kim).

0022-4596/$ - see front matter © 2013 Elsevier Inc. All rights reserved.
http://dx.doi.org/10.1016/j.jssc.2013.11.005

state. It is well known that as the particle size decreases, the surface spins play an important role because of the increase in the surface-to-volume ratio. For nanoparticles, because of the small size of the magnetic material, the coercivity is strongly temperature dependent and follows the thermal activation model.

A multilayer nanowire consists of magnetic segments with dimensions of a few hundred nanometres, which gives rise to interesting magnetic properties at low temperatures that are different from their bulk counterparts [3]. At low temperatures, the anisotropy energy ($E_a = K_{eff}V$) overcomes the thermal energy ($E_{th} = K_BT$) of the nanowires, which increases their magnetic order. As for the coercivity of nanowires with beadlike structures, *Kneller's law* for ferromagnetic nanoparticles is applicable in the temperature range $0 - T_B$, where T_B is the superparamagnetic blocking temperature of the sample. On the other hand, the saturation magnetization follows the modified *Bloch's law* for ferromagnetic nanoparticles [12].

In this work, we report the structure and temperature-dependent magnetic properties of Au–Ni–Au–Ni–Au nanowires fabricated by electrochemical deposition in AAO templates. The structure and morphology were analysed by SEM and TEM. The crystallographic structures and composition of the as fabricated nanowires were confirmed by X-ray diffraction analyses (XRD) and energy-dispersive X-ray spectroscopy (EDX), respectively. In order to check the temperature-dependent magnetic properties of the multilayer nanowires, a superconducting quantum interface device-vibrating sample magnetometer (SQUID-VSM) was used.

2. Materials and methods

In the present work, Au–Ni–Au–Ni–Au nanowires were synthesized by electrochemical deposition into AAO templates with a pore diameter of 100 nm. For this study, the length of the wires is fixed (i.e. 3 μm), while the length of each segment is ~200 nm. The fabrication of multilayer Au–Ni–Au–Ni–Au nanowires is helpful for controlling the length of Ni segments to a few hundred nanometres. For magnetic study of nanowires the direction of the field is very important. In this study the direction of the field is kept along wire long axis. This is because in these nanowires the anisotropy direction is parallel to the length of the wire.

For the growth of nanowires, a DC cell with three electrodes was used. A platinum wire and Ag/AgCl were used as the counter electrode and reference electrode, respectively. One side of the AAO template was made conductive by electron beam (EBM) evaporation of a 200 nm-thick silver layer, which served as the working electrode for the electrochemical deposition.

In order to make the working electrode surface more uniform, a thin sacrificial layer (2 μm) of Ag was electrodeposited. For the synthesis of Au segments, a gold plating solution was used, while a Ni sulphate solution was used for the growth of Ni segments. All electrochemical deposition was carried out at a constant voltage (−0.95 V) for both the Ni and Au segments, and length of each segment was tuned by controlling the charge and time of deposition.

The gold segment length was fixed at both ends to 1 μm, each Ni segment length was controlled to 230 nm, and the sandwiched Au segment length is 180 nm. For the removal of the silver layers (sacrificial and evaporated), the AAO template was treated with nitric acid for 15 min. Multilayer nanowires were separated from the hosting template by dissolving the AAO template into 3 M NaOH solution for 45 min. After releasing nanowires from the template, they were cleaned by centrifugation and rinsing with deionized (DI) water at least 5–7 times. The cleaned nanowires were dispersed on a Si/SiO_2 wafer and dried at 120 °C for 20 min for the structural characterization. Further details of the synthesis process are given in our previous work [13,14].

The morphology of the nanowires was examined by performing SEM and TEM analyses. XRD and EDX were used to determine the crystallographic structure and average chemical composition of nanowires. The magnetic hysteresis $M(H)$ of the as fabricated nanowires were recorded by the SQUID-VSM under a constant applied field of ±3 kOe as the sample temperature was varied from 300 to 2 K. For the magnetic measurements, the wires were left embedded in the AAO template, while for the structural analyses they were released from the template.

3. Results and discussion

Fig. 1 shows SEM and TEM images of Au–Ni–Au–Ni–Au nanowires with average diameters of 100 nm. A TEM image of the uniform Au segment is shown in Fig. 1(a). A multilayer nanowire with two Ni segments sandwiched between the three gold segments is shown in Fig. 1(b). The length of the middle sandwiched gold segment is ~180 nm, and the two Ni segments each have a length of ~230 nm. Fig. 1(c) shows the TEM image of the Ni segments. It can be seen that the Ni segments are not uniform but rather consist of beadlike structures with a bead diameter of ~100 nm stacked on one another to form the nanowire. In Fig. 1(a), it can be seen that the Au segments are uniform and have no beadlike structures like those in the Ni segments.

Fig. 2(a) presents the X-ray diffraction pattern of the multilayer nanowires, in which the observed peaks are indexed according to the standard PCPDF cards for Ni and Au. Quantitative and qualitative analyses of the Au and Ni in the nanowires were performed with the help of the EDX pattern, as shown in Fig. 2(b). The substrate (i.e., Si) and oxygen (O) peaks due to the Si/SiO_2 substrate used for dispersing the nanowires were also observed in the EDX spectra. Thus, both XRD and EDX analyses confirm that

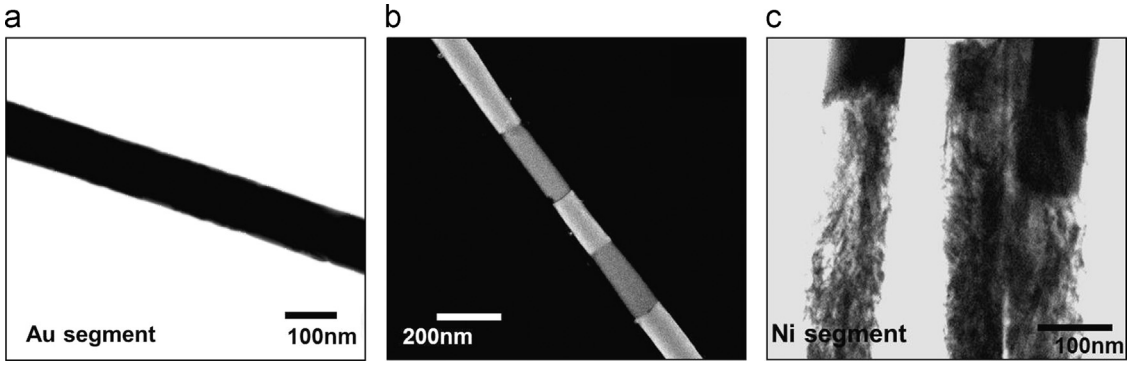

Fig. 1. (a) TEM image of the Au segment showing the uniformity of the Au segments. (b) SEM image of an as-prepared multilayer Au–Ni–Au–Ni–Au nanowire with a Ni segment length of 230 nm and a 180 nm Au segment sandwiched between Ni segments. (c) TEM image of the Ni segment showing the beadlike structure.

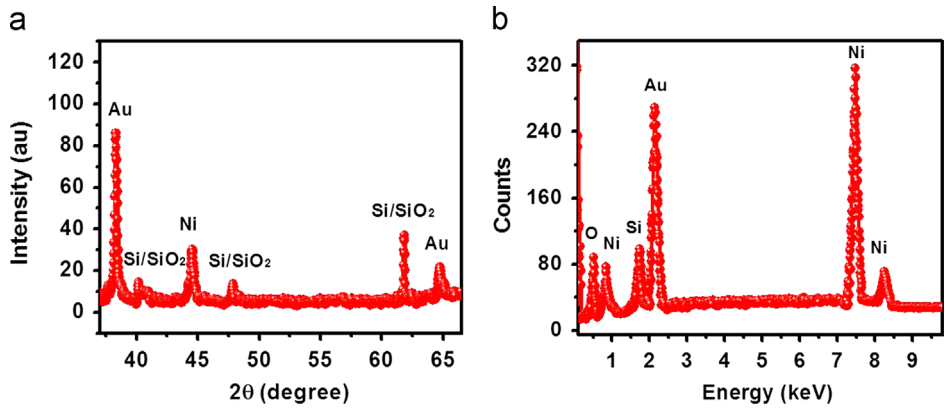

Fig. 2. (a) XRD analyses of wires confirming that the fabricated nanowires have pure phases and are crystalline in nature. (b) EDX spectra showing that the nanowires are composed of Au and Ni without any impurities.

the multilayer nanowires have pure phases and that no impurities were present in the samples.

Magnetic measurements were performed under a field of 3 kOe applied along the long wire axis. Fig. 3(a)–(f) shows the magnetic hysteresis loops $M(H)$ recorded at different temperatures from 2 to 300 K. Multilayer nanowires show ferromagnetic behaviour at room temperature because of the ferromagnetic nature of the Ni segments in the wires, as shown in Fig. 3(f). As the temperature decreases from 300 to 2 K, the anisotropy energy ($E_a = K_{eff}V$) overcomes the thermal energy ($E_{th} = K_BT$), which enhances the magnetic order of the system.

The coercivity (H_c) calculated from the $M(H)$ curves is plotted as a function of temperature from 300 to 2 K in Fig. 4(a). As the temperature decreases, the H_c increases monotonically. It is notable that $H_c(T)$ does not saturate at low temperature (10–2 K), as reported in our previous paper [14]. This could be because our multilayer nanowires are composed of nanoparticles with particle diameters of about 90–100 nm, as mentioned earlier (Fig. 1(c)). Thus, in this case, a simple model of thermal activation of the particle moment over the anisotropy barrier is applicable. In the case of beads (i.e., for a chain of nanoparticles), the structural properties like the volume distribution, randomness of the anisotropy axes and interparticle interactions may also influence the thermal dependence of the coercivity [15]. Therefore, the increase in $H_c(T)$ as the temperature decreases is due to the thermal fluctuations of blocked moments over the anisotropy barrier. It is observed that H_c as function of temperature in the range $0-T_B$ follows Kneller's law for ferromagnetic nanoparticles, which can be written in the form [16]

$$H_c = H_0[(1-T/T_B)^{1/2}] \quad (1)$$

where H_0 is the coercivity at 0 K and T_B is the superparamagnetic blocking temperature. The value of H_0 is 143 Oe, which was approximated by extrapolating the $H_c(T)$ curve toward the field axes. The superparamagnetic blocking temperature (T_B) for these nanowires is 480 K.

The results are fitted to Eq. (1) using the blocking temperature (T_B) as a fitting parameter. In Fig. 4(a), the black curve is the theoretically fitted curve. The experimental results fit the theoretical data very well in the temperature range 2–300 K. It is particularly notable that in the case of multilayer nanowires, the experimental curve agrees for the whole temperature range from 2 to 300 K, while for a single Ni segment these curves deviate in the low-temperature range from 2 to 10 K, where $H_c(T)$ was observed to be saturated, as reported earlier [14]. Similar results for the temperature dependence of the coercivity for Co/Pt multilayers have been reported by Li–F. Liu et al. [9].

Fig. 4(b) shows the temperature-dependent magnetization of the as-prepared multilayer nanowires. In this graph, the magnetization (M) increases as the temperature decreases. The magnetization has a power-law dependence ($T^{3/2}$) on the temperature, which is called Bloch's law and is applicable to bulk materials in the low-temperature range. Bloch's law for bulk ferromagnetic systems can be expressed as [17].

$$M(T) = M(0)[1-(BT)^{\alpha}] \quad (2)$$

Where $M(0)$ is the magnetization at 0 K, B is Bloch's constant, and α is the fitted Bloch's exponent with a value of $\alpha = 3/2$. For nanomaterials, the finite size effects cause the thermal dependence of the magnetization to deviate from the normal Bloch's law, because the magnons with wavelengths larger than the nanostructures' dimensions are difficult to excite. In order to generate spin waves in the materials, a threshold thermal energy is required. Thus, for nanoparticles, the spin wave structure is modified in the form of a power law (T^{α}) with a Bloch's exponent ($\alpha = 2$) larger than its bulk value ($\alpha = 3/2$). The modified Bloch's law for nanoparticles can be expressed as [18–20]

$$M(T) = M(0)[1-(BT)^{2}] \quad (3)$$

In the modified form of Bloch's law, Bloch's constant (B) is the reciprocal of the blocking temperature (T_B) of the nanoparticles ($B = 1/T_B$). Similar results have been observed by Linderoth et al. [21], who observed a modified Bloch's law for amorphous Fe–C nanoparticles with a value of α nearly equal to 2. They argued that the deviation of α from the normal bulk value in case of nanoparticles is due to the finite-size effects and, in particular, the energy gap in the density of states and the lack of magnetic coordination at the surface of the nanoparticles [21]. The value of Bloch's exponent (α) as a function of particle size was determined experimentally by C. R. Alves et al. [19]. They observed a value of α for larger $CuFe_2O_4$ nanoparticles of 3/2, while for smaller nanoparticles α was nearly equal to 2.

In our case, the nanowires are composed of particle-like structures, as shown in Fig. 1(c), and the magnetization as a function of temperature can be fitted theoretically according to the modified Bloch's law. We found that the theoretical curve for the modified Bloch's law with $\alpha = 2$ fully matches the experimental results in the temperature range 2–300 K, as shown in Fig. 4(b). Thus, we conclude that our Au–Ni–Au–Ni–Au nanowires with beadlike structures follow the modified Bloch's law in the temperature range 2–300 K.

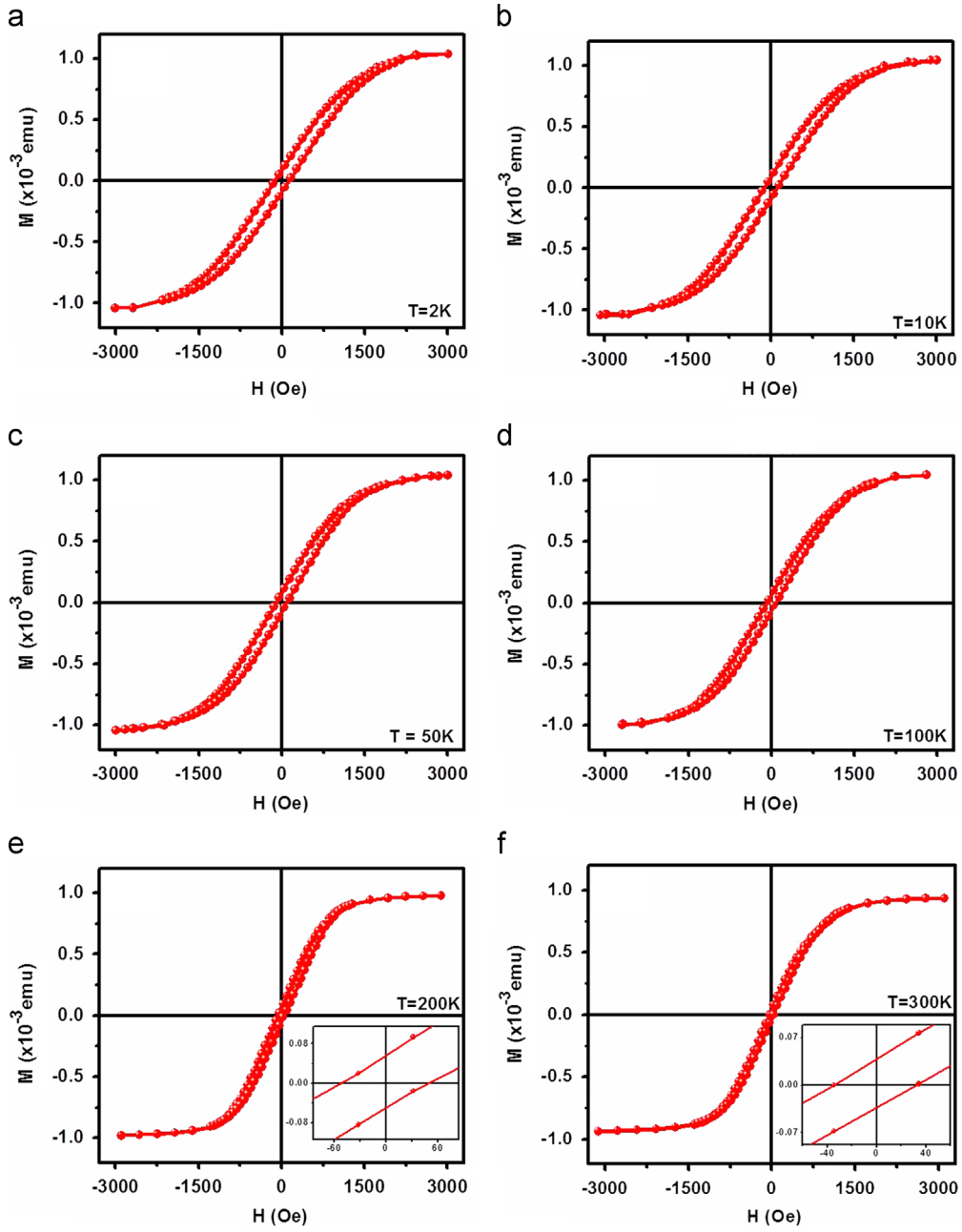

Fig. 3. $M(H)$ loops recorded at temperatures (a) 2, (b) 10, (c) 50, (d) 100, (e) 200, and (f) 300 K under a maximum field of ± 3 kOe. The inset in (e) shows the loop at 200 K magnified at 60 Oe. The inset in (f) shows the $M(H)$ loop at 300 K enlarged at 50 Oe.

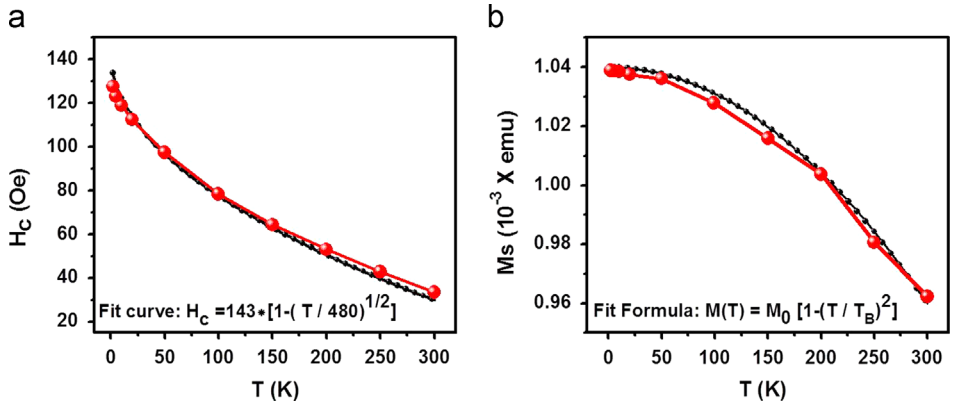

Fig. 4. (a) Coercivity as a function of temperature following the Kneller's law, shown by grey line (red line in web version), while the black line shows the fit curve. (b) Plot of magnetization as a function of temperature in the range 2–300 K. The black line corresponds to the theoretical curve, which is fitted according to modified Bloch's law.

4. Conclusions

Multilayer Au–Ni–Au–Ni–Au nanowires were fabricated by electrochemical deposition into the porous alumina templates with a diameter of 100 nm. The length of each Ni segment was controlled to 200 nm. Structural analyses confirmed the formation of non-uniform Ni segments with pure phase and crystalline structure. The temperature-dependent coercivity $H_c(T)$ of the as-prepared nanowires was found to increase as the temperature decreased from 300 to 2 K. It was found that $H_c(T)$ and the magnetization $M(T)$ follow Kneller's law and the modified Bloch's law, respectively. These results can be explained by taking into account the finite size effects in Au–Ni–Au–Ni–Au nanowires.

Acknowledgments

This work was supported by the World Class University program funded by the Ministry of Education, Science and Technology through the National Research Foundation of Korea (R32-10204) and the IT R&D program of MKE/KEIT (10043398).

References

[1] T.T. Albrecht, J. Schotter, G.A. Kastle, N. Emley, T. Shibauchi, L.K. Elbaum, K. Guarini, C.T. Black, M.T. Tuominen, T.P. Russell, Science 290 (2000) 2126.
[2] T. Nautiyal, T.H. Rho, K.S. Kim, Phys. Rev. B: Condens. Matter 69 (2004) 193404.
[3] S.J. Hurst, E.K. Payne, L. Qin, C.A. Mirkin, Nanostructures 45 (2006) 2672.
[4] S. Kato, H. Shinagawa, H. Okad, G. Kid, K. Mitsuhashi, Sci. Technol. Adv. Mater. 6 (2005) 341.
[5] C.L. Xu, H. Li, G.Y. Zhao, H.L. Li, Mater. Lett. 60 (2006) 2335.
[6] P. Aranda, J.M. Garcia, J. Magn. Magn. Mater. 249 (2002) 214.
[7] J.H. Jeong, S.H. Kim, Y. Choi, S.S. Kim, Phys. Status Solidi C 12 (2007) 4429.
[8] N.V Hoang, S Kumar, Gil-Ho Kim, Nanotechnology 20 (2009) 125607.
[9] Li.F. Liu, W.Y. Zhou, S.S. Xie, O. Albercht, K. Nielsch, Chem. Phys. Lett. 466 (2008) 165.
[10] Y. Liang, L. Zhai, X. Zhao, D. Xu, J. Phys. Chem. B 109 (2005) 7120.
[11] G. Shen, P.C. Chen, Y. Bando, D. Golberg, C. Zhou, Chem. Mater. 20 (21) (2008) 6779;
L. He, W. Zheng, W. Zhou, H. Du, C. Chen, L. Guo, J. Phys. Condens. Matter 19 (2007) 036216.
[12] K Maaz, A. Mumtaz, S.K. Hasanain, M.F. Bertino, J. Magn. Magn. Mater. 322 (2010) 2199.
[13] S. Ishrat, K. Maaz, C. Rong, S.H. Kim, M.H. Jung, Gil-Ho Kim, Curr. Appl. Phys. 12 (2011) 65–68.
[14] S. Ishrat, K. Maaz, Kyu-Joon Lee, M.H. Jung, Gil-Ho Kim, J. Alloys Compd. 541 (2012) 483–487.
[15] O. Iglesias, A. Labarta, X. Batlle, J. Nanosci. Nanotechnol. 8 (2008) 2761.
[16] E.F. Kneller, F.E. Luborsky, J. Appl. Phys. 34 (1963) 656.
[17] X. Battle, M. Garcia del Muro, J. Tejada, H. Pfeiffer, P. Goand, E. Shinn, J. Appl. Phys. 74 (1993) 3333.
[18] F. Bloch, Z. Phys. 61 (1930) 206.
[19] C.R. Alves, M.H. Sousa, H.R. Rechenbrg, G.F. Goya, F.A. Tourinho, J. Depeyrot, J. Metastable Naocryst. Mater. 20-21 (2004) 694.
[20] K. Mandal, S. Mitra, P.Anil Kumar, Europhys. Lett. 75 (2006) 618.
[21] S. Linderoth, L. Balcells, A. Labarta, J. Tejada, P.V. Hendriksen, S.A. Sethi, J. Magn. Magn. Mater. 124 (1993) 269.